Fiber reinforced polypropilene: influence of iPP molecular mass on morphology, crystallization, thermal and mechanical properties

Maurizio Avella, Ramiro Dell'Erba, Ezio Martuscelli

Italian National Agency for New Technologies, Energy and Sustainable Economic Development

http://www.enea.it/en
http://robotica.casaccia.enea.it/index.php?lang=en

This paper is a pre-print. The final paper is available on:

Polymer composites „ Fiber reinforced polypropilene: influence of iPP molecular mass on morphology, crystallization, thermal and mechanical properties“ M. Avella, R. dell’Erba and E. Martuscelli V.17, n.42, (1996).

Fiber Reinforced Polypropylene: Influence of iPP Molecular Weight on Morphology, Crystallization, and Thermal and Mechanical Properties

MAURIZIO AVELLA, RAMIRO DELL'ERBA,** *and* EZIO MARTUSCELLI*

Instituto di Ricerca e Tecnologia delle Materie Plastiche
C.N.R. 80072 Arco Felice (Napoli) Italy

The influence of molecular weight and its distribution on the nucleation density, crystallization, thermal and mechanical behavior of isotactic polypropylene based composites has been investigated. The composites were prepared by compression molding. The ability of carbon and Kevlar fibers to nucleate the polypropylene has been studied during isothermal and nonisothermal crystallization, by optical microscopy and differential scanning calorimetry (DSC), as function of crystallization temperature T_c and iPP molecular weight. Two extreme crystallization conditions were tested: quenching and slow crystallization to obtain crystals and amorphous phases of different structure. The ability of fibers to enhance mechanical properties in polypropylene based composites was examined by tensile tests at room temperature. It was found that nucleation density, crystallization parameters, and the results of tensile tests strongly depend on the molecular weight $\bar{M}w$ of iPP, molecular weight distribution, and thermal history of polypropylene. The numerical values of the nucleation density have been found to strongly depend on the nature of fiber. In fact, Kevlar fiber has shown a better nucleating ability than carbon fiber. The results of tensile tests have been related to the sample morphology. The analysis of fractured specimens also provided useful information about fiber-matrix adhesion.

INTRODUCTION

In previous papers (1, 2) we have reported on the influence of $\bar{M}w$ on the kinetics of polypropylene crystallization. Further, we have studied (3) the influence of thermal history on the tensile behavior of iPP based composites reinforced with carbon and Kevlar fibers, as prepared by compression molding. It was shown that the epitaxial growth of spherulites on the fiber surface (transcrystallinity) can improve the properties of the fiber-matrix interface and consequently those of the composites materials (4, 5).

Moreover, the overall crystallization process (nucleation and growth) is found to strongly depend on both $\bar{M}w$ and thermal treatment (1). We have thus undertaken a study of the influence of $\bar{M}w$ on crystallization and on the thermal and mechanical behavior of iPP based composites. In particular, we have investigated the influence of molecular weight, its distribution and thermal history of iPP nucleation, amount of transcrystallinity, thermal and mechanical behavior, with the aim of quantifying the influence of such factors.

Qualitatively, the nucleating effect was considered by the decreased size and increased number of spherulites compared to the neat polymer and by the possible increase of crystallization temperature evaluated at a constant cooling rate (6). Isothermal crystallization was also performed to measure the decrease in half time of crystallization that is due to the presence of fibers.

EXPERIMENTAL PROCEDURE

Materials

A series of four isotactic polypropylene (iPP) samples, of different molecular weights, supplied by Himont-Italia were used. Their molecular characteristics are reported in *Table 1*. The Kevlar 49 fibers were provided by DuPont (diameter 12–14 μm). The carbon fibers were provided by Marbo Italia S.p.a. (Pan Base type high modulus, 230 GPa, high strain, 1.2 GPa, low strength, diameter 7 to 8 μm). Before use, the fibers were washed in acetone and then overdried at 60°C for 12 hr to remove contaminants from the fiber surface.

* To whom correspondence should be addressed.

** Consorzio sulle Applicazioni dei Materiali Plastici e per i problemi di Difesa dalla Corrosione, via P. Castellino 111, 80100 Napoli, Italy.

Table 1. Molecular Weights Obtained by G.P.C. in Orthodichlorobenzene at 135°C.

Sample	Trade Name	$\bar{M}n$	$\bar{M}w$	$\bar{M}z$	$\bar{M}w/\bar{M}n$
iPP1	Valtec 302	17,200	111,000	545,000	6.4
iPP2	Valtec 298	17,900	178,000	930,000	9.6
iPP3	Valtec Hs010	52,900	361,000	2,332,000	6.8
iPP4	Valtec HI002	91,000	729,000	3,852,000	8.0

Techniques

The apparent melting temperature (T'_m) and the crystallinity index (Xc) for all the iPP samples prepared, both by quenching and isothermally crystallized, were determined by means of a Mettler TA-3000 differential scanning calorimeter (DSC) equipped with a control and programming unit (microprocessor TC-10), operating under nitrogen atmosphere.

The values of T'_m and the apparent enthalpy (ΔH^*) were obtained from the maxima and the area of the melting peaks, respectively. The Xc values of iPP samples were calculated from the following relation:

$$Xc = \Delta H^* / \Delta H^\circ \qquad (1)$$

where ΔH° is the heat of fusion per gram of 100% crystalline iPP, taken as 209 J/g (7).

All the measurements on the samples (about 8–10 mg wt), when not otherwise specified, were performed by using a scan rate of 20°C/min.

The nucleation studies were carried out by utilizing a Leitz polarizing optical microscope equipped with a Mettler hot stage (model FP5), with unit control (model FP52) with a precision of ±0.2°C. Photomicrographs of growing spherulites were taken at time intervals and at crystallization completion to evaluate nucleation density of the spherulites.

The fiber matrix adhesion and morphological investigations were carried out by using a Philips 501 SEM on fracture surfaces obtained by tensile tests at room temperature. The samples for SEM observation were metallized by means of a Polaron sputtering apparatus with Au-Pd alloy.

The mechanical behavior of samples obtained by compression molding was examined. Tests were performed according to ASTM D638 on samples of type IV by using an Instron machine (model 1122) at a cross-head speed of 10 mm/min. The high brittleness of sample iPP1 rendered it impossible for quantitative measurement of its tensile properties with only an overview of its fracture.

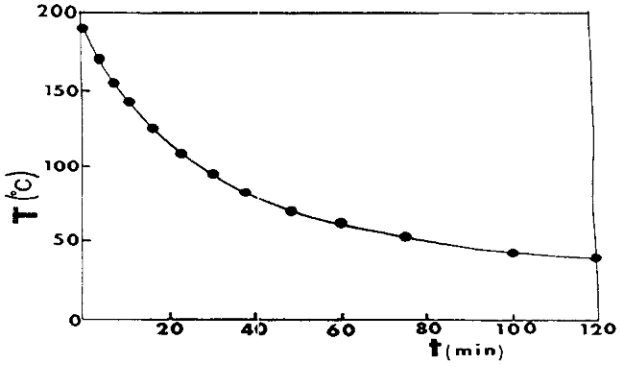

Fig. 1. Experimental curve of cooling rate used for compression molding, S type samples.

Specimen Preparation

The fibers were chopped in short lengths (max ≅ 2 mm) using an electric grinding mill. They were then mixed with polypropylene on a Brabender-like apparatus (Rheocord EC of Haake Inc.) operating at 200°C for 10 min (3).

All prepared composites contained 10 wt% fibers. (The calculated fractions are 5.65 vol% for the carbon fiber composites and 6.80% for the Kevlar fiber composite).

Afterwards, the material was chopped in an electric grinding mill. The mill was placed between two polytetra-fluoroethylene sheets and laterally contained in a 1.0-mm-thick steel frame. The system was inserted within the plates of hydraulic press heated at 190°C and kept for 10 min without applied pressure, allowing for complete melting. After this period, a pressure of 10 MPa was applied for 5 min.

By use of the following two procedures, two different classes of sample were prepared: 1) fast cooling by quenching in ice/NaCl (–20°C); and 2) slow cooling to

Table 2. Thermal Treatment of Samples and Classification Code Used.

Samples	Code	Thermal Treat.
iPP1	iPP1S	Slow*
iPP1/10%	iPP1SC	
iPP1/10%	iPP1SK	
iPP1	iPP1F	Quenched**
iPP1/10%	iPP1FC	
iPP1/10%	iPP1FK	
iPP2	iPP2S	Slow
iPP2/10%	iPP2SC	
iPP2/10%	iPP2SK	
iPP2	iPP2F	Quenched
iPP2/10%	iPP2FC	
iPP2/10%	iPP2FK	
iPP3	iPP3S	Slow
iPP3/10%	iPP3SC	
iPP3/10%	iPP3SK	
iPP3	iPP3F	Quenched
iPP3/10%	iPP3FC	
iPP3/10%	iPP3FK	
iPP4	iPP4S	Slow
iPP4/10%	iPP4SC	
iPP4/10%	iPP4SK	
iPP4	iPP4F	Quenched
iPP4/10%	iPP4FC	
iPP4/10%	iPP4FK	

* Samples slowly cooled to 25°C following the temperature-time cooling of *Fig. 1.*
** Samples rapidly cooled to –20°C (ice/NaCl mixture).

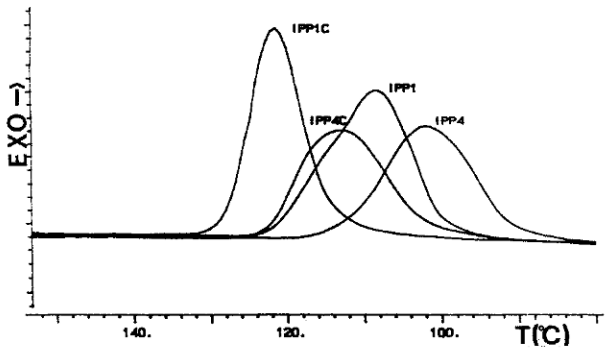

Fig. 2. Nonisothermal crystallization curves (20°C/min) for iPP1, iPP4, iPP1C, and iPP4C samples.

room temperature following the temperature-time cooling curve shown in *Fig. 1*.

Twenty-four types of samples were prepared. The samples have the following codes: iPP1S, iPP2S, iPP3S, iPP4S, iPP1F, iPP2F, iPP3F, iPP4F, for the neat polymer where the iPPs are numbered in increasing $\bar{M}w$. The letters F or S stand for fast or slow cooling rates, as explained in *Table 2*.

The code of composites reinforced by carbon fibers are: iPP1SC, iPP2SC, iPP3SC, iPP4SC, iPP1FC, iPP2FC, iPP3FC, iPP4FC, where the letter C stands for carbon fiber reinforcement.

Finally the code for Kevlar composites are: iPP1SK, iPP2SK, iPP3SK, iPP4SK, iPP1FK, iPP2FK, iPP3FK, iPP4FK, where the letter K stands for Kevlar fiber reinforcement.

For microscope analysis (8), all samples were preparing by fixing a single fiber onto a glass microscope slide with a small quantity of polypropylene; the temperature was raised to the melting temperature of iPP, and then a glass cover was pressed to produce a thin film sample with the fiber embedded in the polymer.

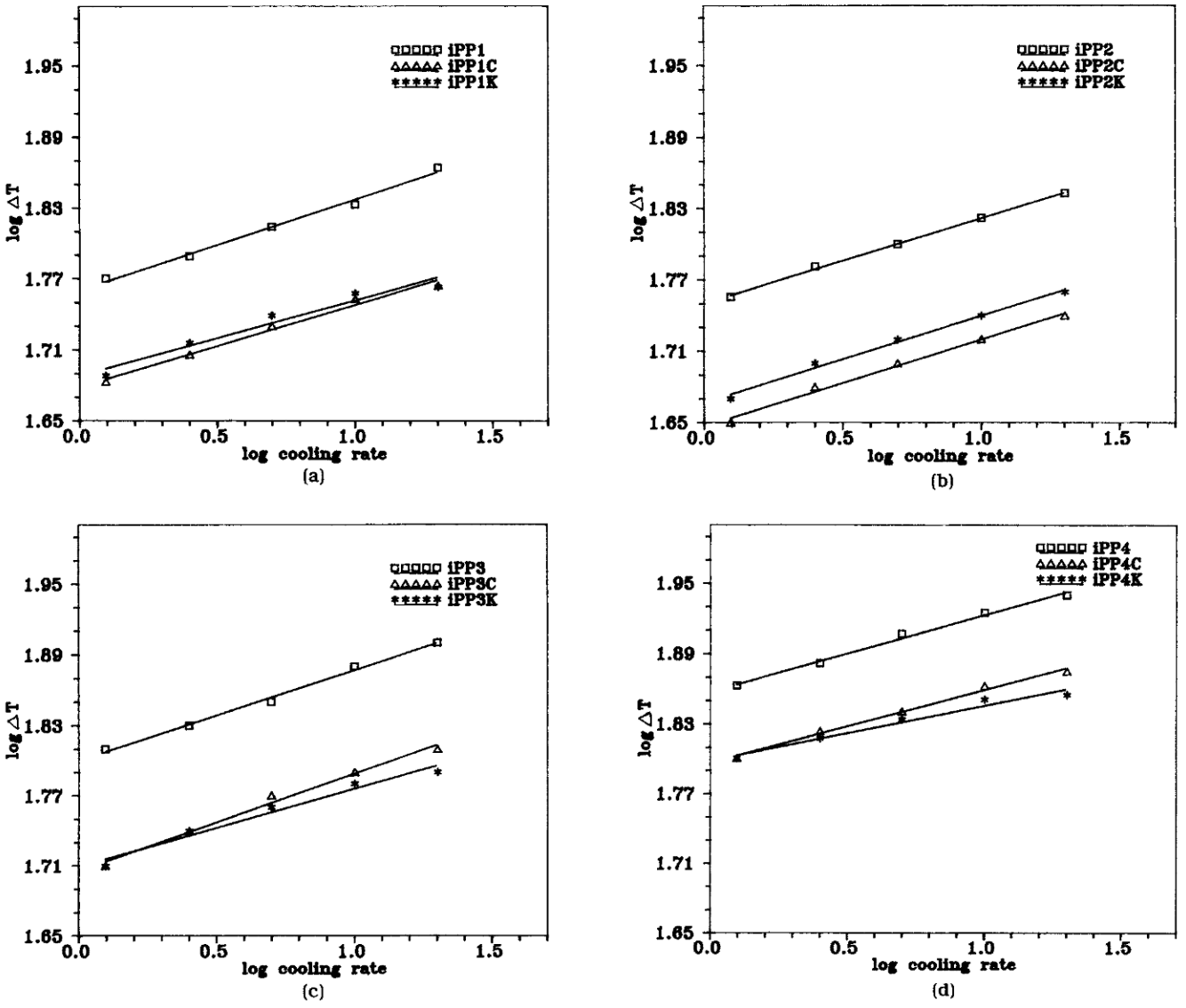

Fig. 3. Experimental correlation between log ΔT (effective supercooling) and log cooling rate. a) iPP1; b) iPP2; c) iPP3; d) iPP4. □ neat; Δ carbon; • Kevlar.

On a Mettler hot stage, the following procedure was used: the sample was heated at 190°C and held for 10 min under N_2 atmosphere to destroy any trace of crystallinity; then, the samples were rapidly lowered (30°C/min) to a prefixed crystallization temperature (*Tc*) and allowed to crystallize. The temperatures used were 125, 129, and 133°C, to entirely cover the maximum common range of isothermal crystallization.

The nucleation rates on the fiber surface and in the bulk polypropylene were measured by counting the number of spherulites nucleated, at prefixed time intervals, in a given area of the specimen, as crystallization proceeded isothermally. This area was taken, in the case of the fiber, as the columnar area of transcrystallinity band when the nucleation rate on the fiber dropped to zero.

The high nucleation rate of the iPP1SK sample made it impossible to measure the nucleation density.

RESULTS AND DISCUSSION

Nonisothermal Crystallization

The effect of nucleation on carbon and Kevlar fibers on the crystallization of iPP has been studied by nonisothermal experiments. The specimens were heated from 30 to 200°C at a scan rate of 20°C/min and held for 10 min. The samples were then cooled to 30°C by using a prefixed scan rate. An additional second fusion run to 200°C was carried out.

The average values of apparent melting temperature (T_m'), the crystallinity percent (*Xc*), determined as the ratio of the apparent fusion enthalpy ΔH_m^* to the melting enthalpy ΔHm of a sample of 100% of crystallinity [taken as 209 J/g (7)], and the temperature of the crystallization peak (*Tc*) are reported for each run in *Table 3a* and *3b* by using five different cooling rates.

From these data the following emerges: i) In the first fusion cycle, the crystallinity of iPP decreased with increasing $\bar{M}w$ for plain iPP and its composites; no substantial difference in these values of *Xc* was observed between plain iPP and its composites. ii) Run II (nonisothermal crystallization) showed that, in the case of composites, the crystallization peak's temperature is shifted toward higher values than that of neat iPP, as can be seen from the thermograms in *Fig. 2*. This behavior agrees with a strong nucleation ability of the fibers. Moreover, the nucleating ability of the fibers does not seem to be influenced by the molecular weight of iPP. iii) Run III (second melting), after nonisothermal crystallization, has shown a decrease in crystallinity index with an increase of $\bar{M}w$, as found in the I run.

In a nonisothermal crystallization process, on cooling, polymers crystallize over a range of supercooling (9) $\Delta T (\Delta T = T_m^\circ - Tc$ where T_m° is the equilibrium melting temperature, already calculated in Ref. 1. As a matter of fact, it is known that samples with a high nucleation density crystallize at lower undercoolings than samples with a low nucleation density (10).

In *Figs. 3a* through *3d*, the correlation between the log of ΔT and the log of the cooling rate for the samples of fixed $\bar{M}w$ is shown. From the *Figures*, it is possible to conclude that composites are characterized by values of ΔT that are lower than those of plain iPP. Further, the undercoolings' ΔT increase with the cooling rate. No differences between the composites with Kevlar and carbon fiber are observed. The slopes of straight lines of *Figs. 3a* through *3d*, for plain iPP and composites, indicate that sensitivity to the cooling rate is the same for neat polymer and composites.

Isothermal Crystallization

To study isothermal crystallization, plots at constant *Tc* of the weight fraction (*Xt*) of material crystallized at time *t* vs. time were created. From these plots, the half times of crystallization ($t0.5$) for all the samples were obtained; the values of $t0.5$, for neat iPP and for iPP crystallized from Kevlar composites are reported, at fixed *Tc*, as function of $\bar{M}w$ in *Figs. 4a* and *4b*, respectively. These *Figures* show that, for a given *Tc*, the values of $t0.5$ increase with increasing $\bar{M}w$ of iPP both in plain iPP and in composites.

The reinforced iPP samples show values of $t0.5$ much lower than corresponding plain iPP, in spite of a

Table 3a. Apparent Melting Point, Crystallinity Index, and Crystallization Peak of Samples.

	I RUN		cool.rate: 20°C/min				cool.rate: 10°C/min			
Code	Tm (C)	Xc (%)	Tc (C)	Xc (%)	Tm (C)	Xc (%)	Tc (C)	Xc (%)	Tm (C)	Xc (%)
iPP1S	166.8	47	110.4	44	160.0	43	114.4	45	161.0	43
iPP1SC	165.5	49	124.6	46	157.6	44	126.9	48	158.1	45
iPP1SK	165.0	46	122.2	45	160.6	42	124.9	45	160.6	43
iPP2S	162.3	44	107.8	41	161.0	39	111.1	43	161.0	40
iPP2SC	162.3	44	122.1	43	158.4	39	124.2	43	161.6	35
iPP2SK	163.1	44	121.8	43	161.5	42	124.2	44	161.5	43
iPP3S	164.5	38	105.0	38	161.8	36	109.5	38	160.4	38
iPP3SC	167.9	41	120.2	41	161.7	38	123.3	41	165.0	40
iPP3SK	165.3	39	120.7	39	163.1	38	124.3	41	163.4	39
iPP4S	161.7	38	104.5	37	157.9	35	108.4	38	157.9	34
iPP4SC	161.8	37	114.4	39	159.7	37	118.3	40	158.1	36
iPP4SK	159.8	40	119.7	39	158.2	38	122.4	41	157.6	36

Table 3b. Apparent Melting Point, Crystallinity Index, and Crystallization Peak of Samples.

	I RUN		cool.rate: 5°C/min				cool.rate: 2.5°C/min				cool.rate: 1.25°C/min			
Code	Tm (C)	Xc (%)	Tc (C)	Xc (%)	Tm (C)	Xc (%)	Tc (C)	Xc (%)	Tm (C)	Xc (%)	Tc (C)	Xc (%)	Tm (C)	Xc (%)
iPP1S	166.8	43	116.4	46	157.3	41	119.9	46	158.7	44	123.9	47	159.5	45
iPP1SC	165.5	45	127.6	47	159.6	44	130.5	47	161.1	45	133.8	47	161.2	47
iPP1SK	165.0	43	127.5	45	161.4	43	129.8	47	161.4	44	133.1	47	162.0	45
iPP2S	162.3	43	115.4	45	157.9	43	118.3	45	157.8	43	121.6	46	158.9	45
iPP2SC	162.3	43	127.7	44	159.5	43	130.5	46	159.6	44	133.1	48	161.2	46
iPP2SK	163.1	41	126.0	43	161.5	40	129.1	44	163.0	43	131.6	46	162.7	45
iPP3S	164.5	40	113.5	42	162.3	40	117.2	42	160.5	42	121.1	44	160.4	40
iPP3SC	167.9	40	126.9	42	161.1	39	129.9	43	162.6	40	133.1	43	163.6	40
iPP3SK	165.3	42	126.4	44	162.7	39	129.3	43	162.7	41	131.7	44	163.6	40
iPP4S	161.7	37	111.7	39	159.8	37	114.8	41	158.2	37	117.5	41	158.1	38
iPP4SC	161.8	40	122.5	41	158.9	39	125.6	42	158.9	38	129.5	42	159.9	39
iPP4SK	159.8	39	124.5	41	158.2	39	126.9	41	158.2	40	130.2	40	159.4	39

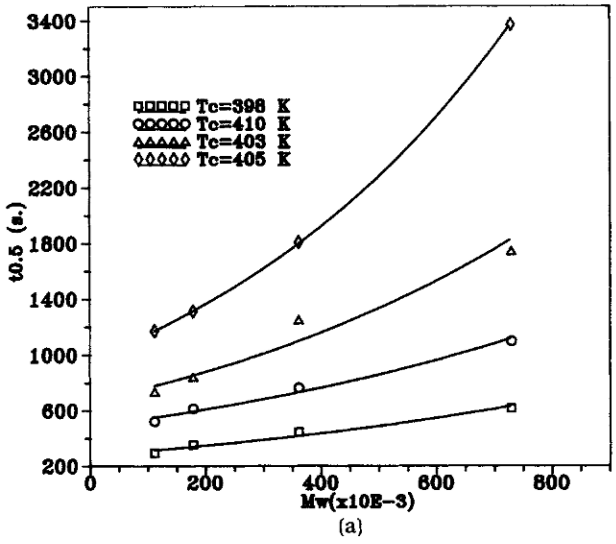

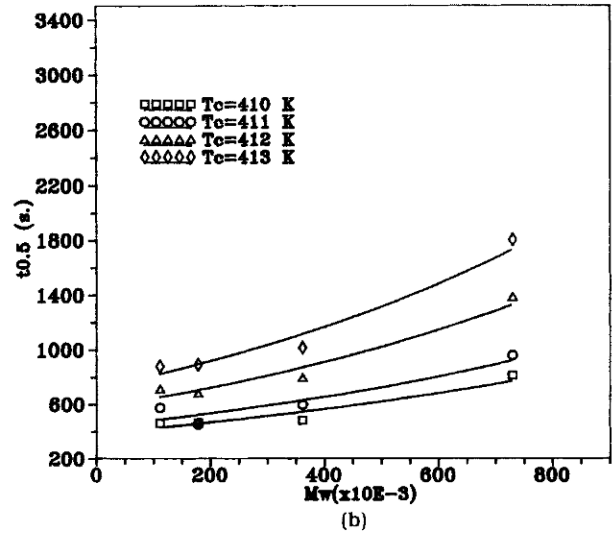

Fig. 4. Half time of crystallization of neat polymer (a) and Kevlar composites (b) samples vs. Mw at fixed Tc.

higher crystallization temperature, owing to the nucleating ability of the fibers (see also *Table 4*).

The values of $t0.5$ for composites was almost independent of the fiber used.

The analysis of the crystallization kinetics, for each Tc, has been carried out using the Avrami equation (11):

$$1 - Xt = e^{-Kt} \tag{2}$$

where K is the kinetic rate constant and n is a parameter depending on the geometry of the growing crystals and on the nucleation process. The values of n and K were calculated from the slope and the intercept, respectively, of the straight line obtained by plotting the quantity $\log(-\ln(1 - Xt))$ against $\log t$.

Table 4 gives the values of K,$t0.5$ and n for all values of Tc investigated. The Avrami exponent n for plain iPP ranges around 2. This would indicate heterogeneous nucleation with bidimensional growth of crystals (11–13). On the contrary, for iPP based composites, the exponent n ranged ~ 3, as found previously (3). Such a finding suggests a heterogeneous nucleated three-dimensional growth of crystals, probably induced by the presence of fibers.

Nucleation and Transcrystallinity Phenomena

In a previous work (8), a study on isothermal crystallization from the melt of iPP showed that the presence of carbon and Kevlar fibers increases the overall nucleation density of spherulites, and the occurrence of transcrystallinity on fiber surface was extensively observed.

The same experiment was then performed using iPP samples with different molecular weights to study the influence of $\bar{M}w$ on nucleation in the bulk and on fiber surfaces and the eventual occurrence of transcrystallinity. *Figures 5a* through *5c* report the number of visible spherulites at complete crystallization for unit area, measured with an optical microscope, in the bulk iPP (*Fig. 5a*), on the carbon fiber (*Fig. 5b*), and on the Kevlar fiber (*Fig. 5c*) vs. crystallization temperature for all the samples with fixed $\bar{M}w$. In the case of iPP1 Kevlar composites (lowest $\bar{M}w$), it was not possible to measure the number of spherulites for unit area because of the too-high nucleation rate.

Table 5 gives the numerical values of calculated nucleation density. It can be pointed out that trans-

Table 4. Crystallization Temperature, Half Time of Crystallization, Avrami Exponent and Kinetic Rate Constant.

Code	Tc (K)	t0.5 (s)	n	Kn (s ^ n)	average n
Plain iPP					
iPP1S	398	293	1.8	2.5E-05	1.9
	401	522	2.0	3.1E-06	
	403	733	2.0	1.7E-06	
	405	1170	2.0	4.7E-07	
iPP2S	398	353	1.8	1.8E-05	1.9
	401	614	2.1	9.7E-07	
	403	841	1.9	1.9E-06	
	405	1310	1.9	1.1E-06	
iPP3S	398	445	2.0	4.8E-06	2.0
	401	764	1.9	2.2E-06	
	403	1249	2.4	1.9E-08	
	405	1806	1.8	1.1E-06	
iPP4S	398	614	2.4	1.6E-07	2.3
	401	1096	2.5	2.2E-08	
	403	1740	2.5	8.0E-09	
	405	3368	2.0	9.2E-08	
Carbon reinforced iPP					
iPP2SC	410	422	2.7	6.4E-08	2.7
	411	508	2.6	6.0E-08	
	412	619	2.7	2.6E-08	
	413	724	2.8	7.8E-09	
iPP2SC	410	591	2.6	5.6E-08	2.6
	411	722	2.5	6.4E-08	
	412	884	2.5	3.2E-08	
	413	1055	2.8	3.1E-09	
iPP3SC	410	555	2.6	7.0E-08	2.5
	411	673	2.4	1.1E-07	
	412	819	2.4	7.1E-08	
	413	1020	2.8	2.0E-09	
iPP4SC	410	1184	2.5	1.4E-08	2.5
	411	1402	2.5	9.4E-09	
	412	1673	2.4	1.3E-08	
	413	1916	2.7	9.5E-10	
Kevlar reinforced iPP					
iPP1SK	410	460	2.6	9.9E-08	2.6
	411	574	2.7	2.6E-08	
	412	714	2.7	1.9E-08	
	413	879	2.7	9.6E-09	
iPP2SK	410	463	2.5	1.6E-07	2.5
	411	543	2.6	6.9E-08	
	412	682	2.6	4.1E-08	
	413	891	2.6	1.8E-08	
iPP3SK	410	481	2.6	9.4E-08	2.4
	411	596	2.3	2.4E-07	
	412	798	2.4	7.5E-08	
	413	1013	2.4	6.0E-08	
iPP4SK	410	813	2.1	4.1E-07	2.3
	411	958	2.5	3.4E-08	
	412	1384	2.3	4.1E-08	
	413	1802	2.4	1.5E-08	

crystallinity regions were found in the whole *Tc* range for Kevlar-reinforced composites, whereas in carbon reinforced composites it occurs only at the lowest *Tc*.

These findings indicate that for the *Tc* range investigated, the nucleation density on the fiber, both Kevlar and carbon, is higher than the nucleation in the bulk. Further, the nucleation on Kevlar fiber is always higher than the nucleation measured on the carbon fiber; in fact, Kevlar fiber shows a better nucleating ability and a larger number of transcrystallinity regions, while the carbon fiber shows extensive transcrystallinity only at the lowest *Tc* value. We may suppose that this result can be ascribed to a different geometrical structure of the fibers—the Kevlar fiber

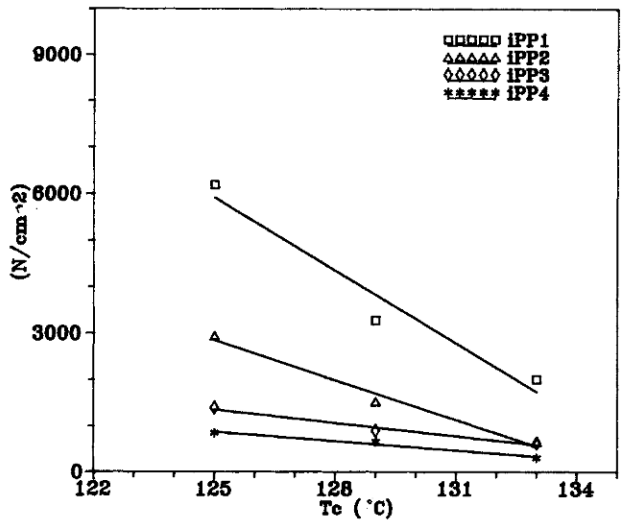

(a)

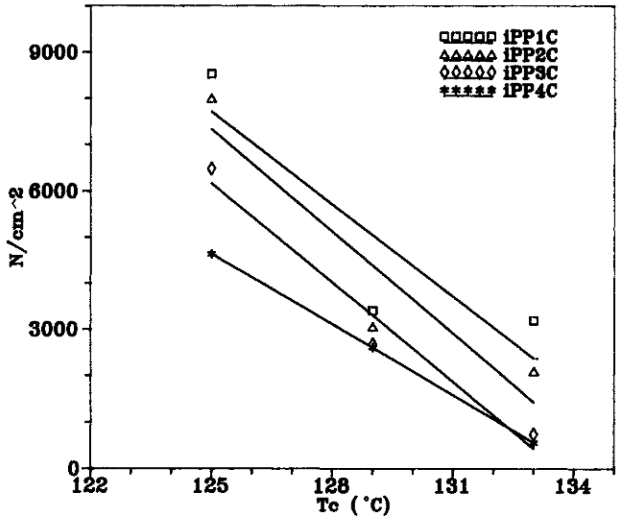

(b)

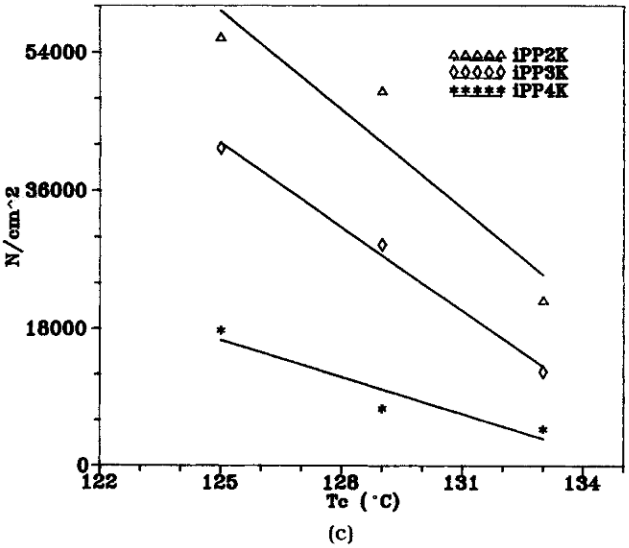

(c)

Fig. 5. Variation of nucleation density (N) vs. Tc; a) iPP; b) carbon reinforced iPP; c) Kevlar reinforced iPP.

Table 5. Nucleation Density Values.

Code	Tc = 125°C	Tc = 129°C	Tc = 133°C
	N/cm^2	N/cm^2	N/cm^2
iPP1S	6200	3300	2000
iPP1SC	*8500	3400	3200
iPP1SK	—	—	—
iPP2S	2900	1500	650
iPP2SC	*8000	3000	2100
iPP2SK	*56,000	*49,000	*22,000
iPP3S	1400	900	600
iPP3SC	*6500	2700	750
iPP3SK	41,500	29,000	12,300
iPP4S	850	1350	300
iPP4SC	*4600	2600	550
iPP4SK	*18,000	*7500	*4800

* = low transcrystallinity.

probably presents a larger number of physical irregularities on its surface, which can act as nucleating sites for iPP crystals (8).

Moreover, for a given molecular weight, the nucleation density on both the fibers and in the bulk decreases with increasing *Tc*, as shown in *Figs. 5a* through *5c*.

The influence of $\bar{M}w$ on nucleation density can be more easily seen in *Figs. 6a* through *6c*, where reported are the nucleation density in the bulk (*Fig. 6a*), nucleation density on carbon fiber (*Fig. 6b*), and nucleation density on Kevlar fiber (*Fig. 6c*) vs. $\bar{M}w$, at constant *Tc*. It can be observed that the *Mw* has a strong influence both on nucleation on the fibers and nucleation in the bulk; in fact, the nucleation density, on the fibers and in the bulk, at constant values of *Tc* was drastically lowered by increasing $\bar{M}w$. This behavior is enhanced by decreasing *Tc*, in accordance with the previous data that show a stronger influence on the *Tc* of the lower-molecular-weight sample.

Finally, the strong influence of *Mw* on the nucleation of iPP is independent of its molecular weight distribution (*MWD*); in fact, samples having the same *MWD* (iPP1 and iPP3) but different $\bar{M}w$ present very different nucleation density values.

Tensile Properties

Figures 7a and *7b* are examples of stress-strain curves, corresponding to samples iPP2S and iPP4S, of different molecular weight iPP. The remarkable difference for the plain and composite iPP samples can be ascribed both to the presence of the fibers and the influence of different molecular weights. To have an understanding of the effect of $\bar{M}w$ on tensile properties, we consider also the presence of tie-molecules in the polymer structure. In fact, adjacent lamellae and spherulites are bridged by interspherulitic molecular links, called tie-molecules, which act as local transducers of stress among lamellae and spherulites and hence are able to control the deformation.

The concentration of tie-molecules is related to the crystallization condition and decreases (14) markedly with decreasing molecular weight and increasing *Tc*. Therefore, when the number of tie-molecules is de-

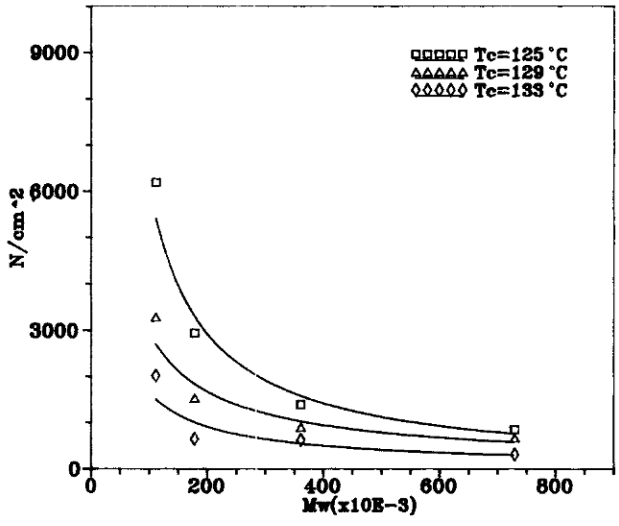

(a)

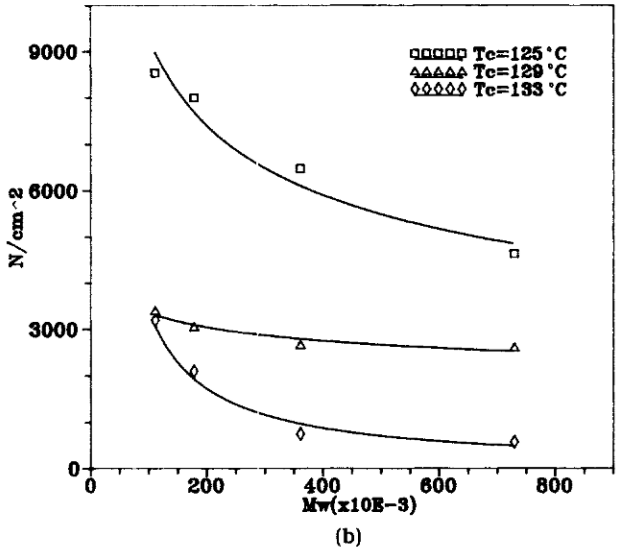

(b)

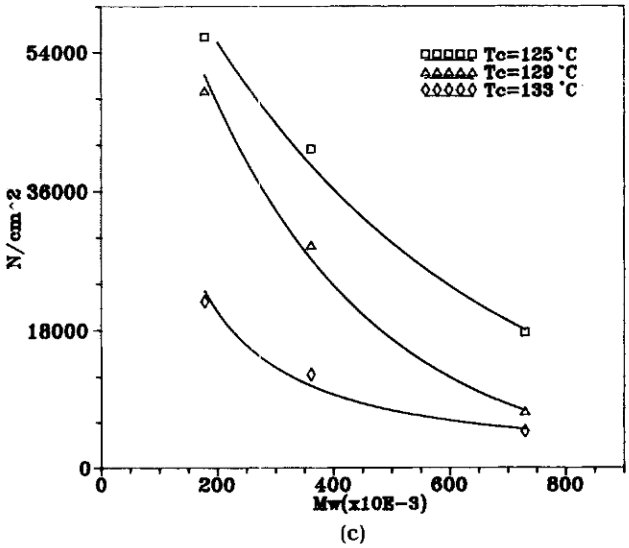

(c)

Fig. 6. Variation of nucleation density (N) vs. Mw. a) iPP; b) carbon reinforced iPP; c) Kevlar reinforced iPP.

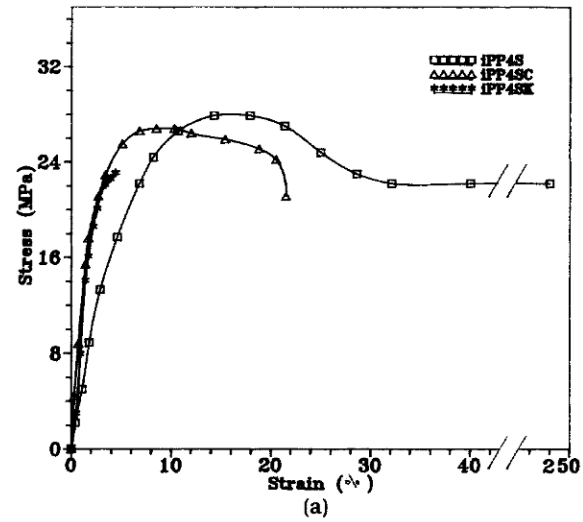

(a)

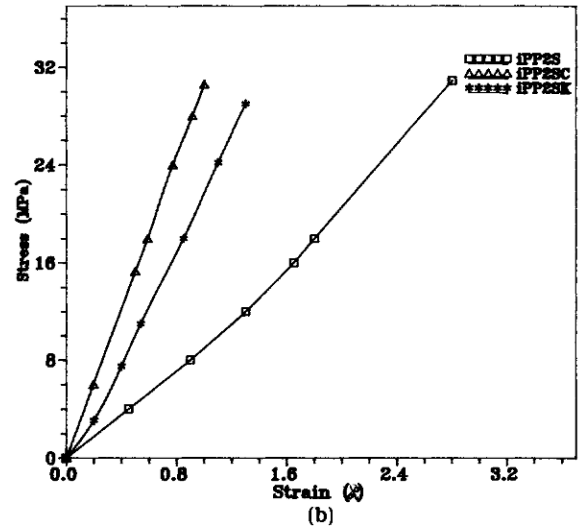

(b)

Fig. 7. Stress-strain curves to failure of a) iPP2S; b) iPP4S. □ iPP; Δ carbon composites; • Kevlar composites.

creased, the polymer becomes physically less interconnected, and hence the applied load becomes concentrated at increasingly fewer sites at the surface of crystallites, producing large stress concentrations, so a more brittle behavior is expected. As already described, the Kevlar and carbon fibers influence the nucleation of spherulites of iPP and consequently can influence its mechanical properties.

Further, to obtain composites with good properties, it is important to realize good adhesion between fiber and matrix to improve the stress transmission from the matrix to the fibers by the interface. *Table 6* gives the results relative to the tensile tests. This *Table* shows:

i) Brittleness increases with decreasing $\bar{M}w$ and that the composites show an increase of Young's modulus, E, with respect to the plain iPP; this increase is stronger for samples containing carbon fibers than for samples containing Kevlar fibers.

Table 6. Tensile Results (ASTM D638; Test Speed = 10 mm/min).

Code	E (GPa)	ε (%)	σ (MPa)
iPP2S	2.4	2.8	32.2
iPP2F	1.0	9.8	30.0
iPP2SC	3.2	1.0	28.4
iPP2FC	1.4	3.9	27.5
iPP2SK	2.8	1.4	28.3
iPP2FK	1.1	5.6	25.2
iPP3S	1.1	7.8	34.7
iPP3F	0.9	720.0	33.6
iPP3SC	1.6	5.8	30.6
iPP3FC	1.2	31.0	22.6
iPP3SK	1.3	4.1	27.4
iPP3FK	0.9	7.6	24.4
iPP4S	0.7	250.0	22.4
iPP4F	0.7	>800	16.4
iPP4SC	1.3	19.0	25.6
iPP4FC	1.0	240.0	18.6
iPP4SK	1.3	4.4	23.7
iPP4FK	0.9	8.0	24.5

At fixed $\bar{M}w$, the increase of modulus is more remarkable for samples of type S rather than quenched samples; this is probably because slowly cooled material retains less internal stress and is capable of creating a strong fiber-matrix adhesion with respect to quenched samples.

The Young's moduli, calculated from the initial slope of stress-strain curves vs. molecular weight, are shown in *Fig. 8a* (S samples) and *8b* (F samples). The rigidity decreased with increasing $\bar{M}w$; this suggests a decrease on the tie-molecules with decreasing $\bar{M}w$, and consequently a lower degree of interconnections between spherulites; further, the increase of modulus attributable to the presence of fibers is stronger for higher Mw samples.

The quenched samples (*Fig. 8b*) show similar trends, but with a lower sensitivity to $\bar{M}w$ and the presence of fibers, probably owing to worse fiber-matrix adhesion, with respect to S samples (as will be later shown by the morphological analysis) and owing to the higher degree of interspherulitic links; in fact, during the slow crystallization of samples, defective and noncrystallizable molecules that usually form tie-molecules are rejected from the growing fronts of spherulites and thus do not bridge the spherulitic structure.

ii) The strength at break, σb, seems to decrease in composite materials with respect to plain iPP; as found in the case of modulus, a slower cooling of the sample involves a greater strength at break, compared with those of corresponding quenched samples.

iii) The elongation value at break εb showed a strong dependence on $\bar{M}w$ and thermal treatment; also in this case, the microspherulite morphology of quenched samples probably makes able them to support a stronger elongation before the break. All the composite materials have shown an εb much less than that of plain iPP; this behavior is enhanced with increasing $\bar{M}w$. From *Table 6* it is also evident that a high $\bar{M}w$ sample exhibits a more ductile behavior with respect to a lower $\bar{M}w$; further, the higher molecular weight composites have such a ductile behavior that some samples (iPP4FC, iPP3FC) evince yielding points typical of corresponding plain iPP before break.

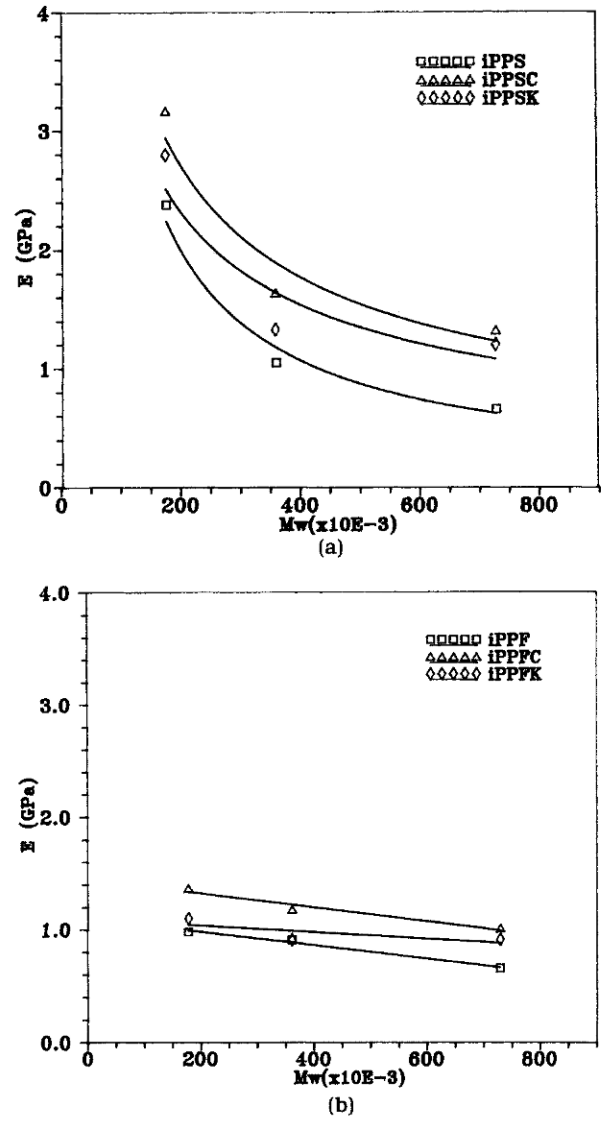

*Fig. 8. Variation of Young's modulus versus Mw; a) S-samples; b) F-samples. □ iPP; Δ carbon composites; * Kevlar composites.*

The εb of carbon composites is generally higher than that of the Kevlar composites.

The morphology of fractured specimens was examined by SEM to investigate the relationship between the mechanical properties and the resulting microstructure of iPP based composites. In *Figs. 9a–12b* SEM micrographs of failure surfaces of plain iPP samples are shown; all the pictures were taken in the region of the crack.

The higher moduli and low elongation at break for the lower molecular weight samples show a morphology typical of a material that has undergone a brittle

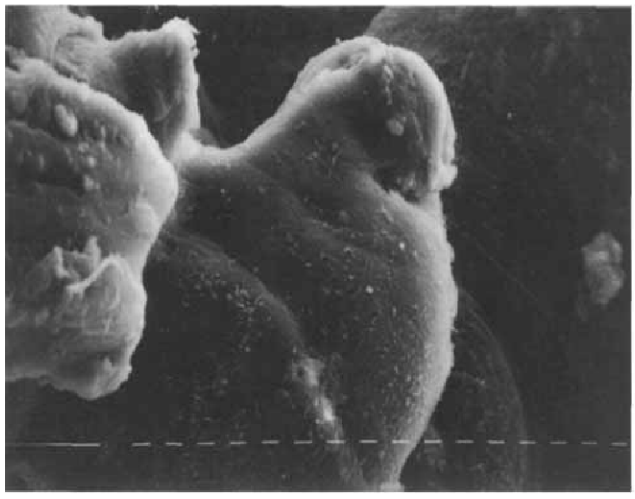

(a)

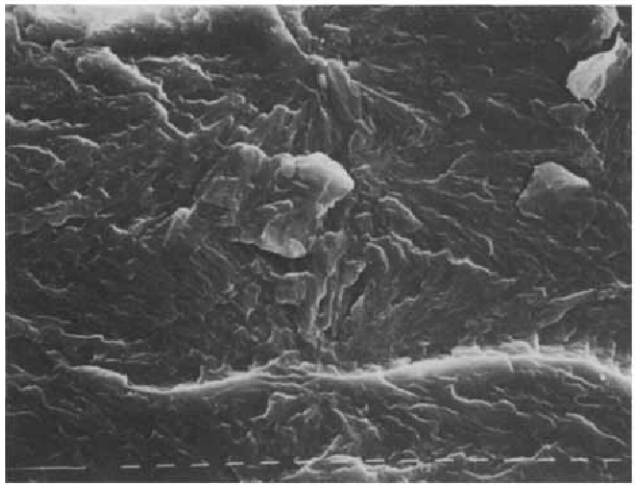

(b)

Fig. 9. Scanning electron micrographs of fractured surface of iPP samples. a) iPP1S 320×; b) iPP4S; 320×.

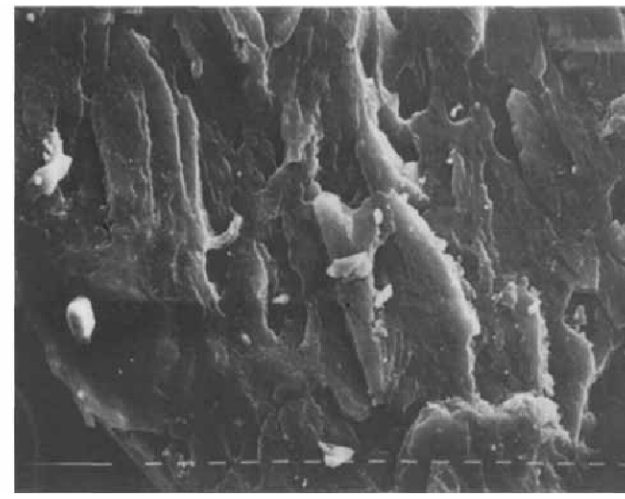

(a)

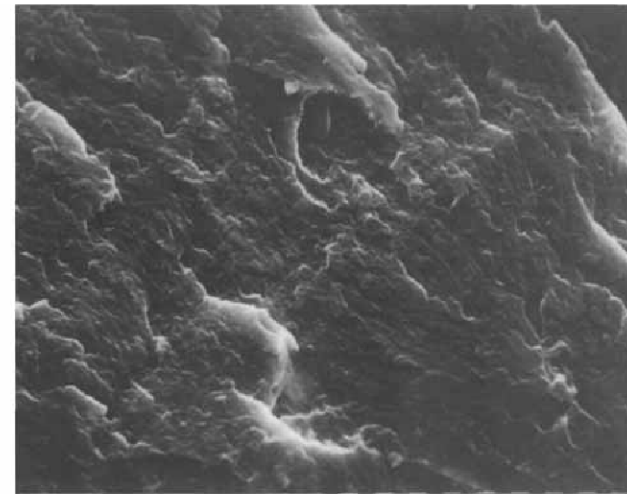

(b)

Fig. 10. Scanning electron micrographs of fractured surface of iPP samples with different crystallization procedures: a) iPP2S 320×; b) iPP2F 320×.

mode of failure and only a very limited plastic flow process before the breakage; on the contrary, the higher Mw samples show a large zone where the sample is plastically deformed (compare *Fig. 10a* and *10b*, where the fracture surfaces of samples iPP1S and iPP4S are shown). This difference in the mechanical behavior, with $\bar{M}w$ is greater in the S samples, owing to the different microstructure with respect to F samples (3); in fact, the slowly cooled iPP presents a large spherulite morphology, and consequently, it probably has only a few interspherulitic links that bridge the spherulites. On the contrary, the fast-cooled iPP presents smaller spherulites with respect to the S samples, and it is possible to suppose a high degree of connections among the spherulites and consequently a better possibility of transferring the stress before the break.

Previous studies (15–17) have reported that ductility and yield strength are improved with decreasing spherulite size; in *Fig. 10a* and *10b*, in which the samples iPP2S and iPP2F are shown, a considerable difference in the "mackerel" (crazing zones) dimension is observed, indicating more ductility of F samples with respect to S samples.

The iPP reinforced by carbon fibers (*Figs. 11a,b,c*), both in F and in S samples, shows more fiber alignment with increasing Mw, which indicates a larger plastic flow of the matrix along the fibers before the break. This can be interpreted as an improvement the fiber-matrix adhesion with increasing $\bar{M}w$, because, of again, the enhancing connection between spherulites with increasing $\bar{M}w$ and the nucleating ability of the fiber.

The samples iPP3SC and iPP4SC yielded before break, and this is observable in the large zone of plastic deformation visible in *Fig. 11b* and *Fig. 11c*, which show that before breakage, the matrix has flowed along the fibers without debounding from them. For the Kevlar composites and the observations by SEM micrographs (see *Figs. 12a* and *12b*), there is a stronger fiber-matrix adhesion in the case of higher $\bar{M}w$. Indeed, the sample iPP4SK shows many broken and

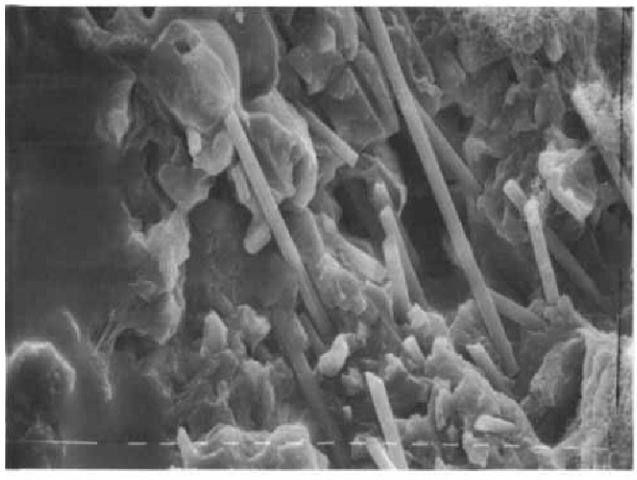

(a)

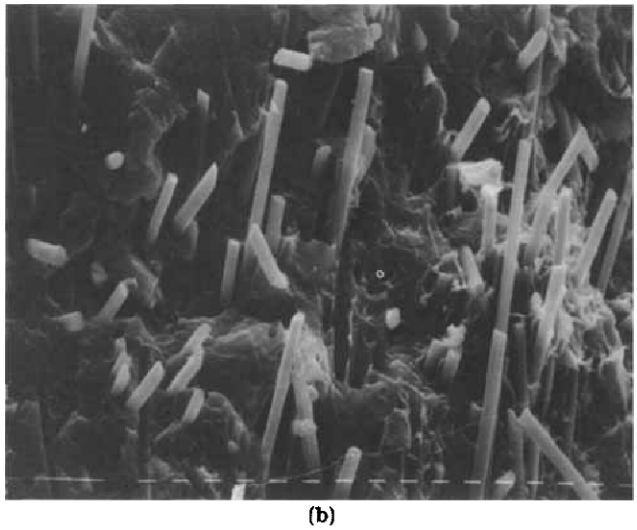

(b)

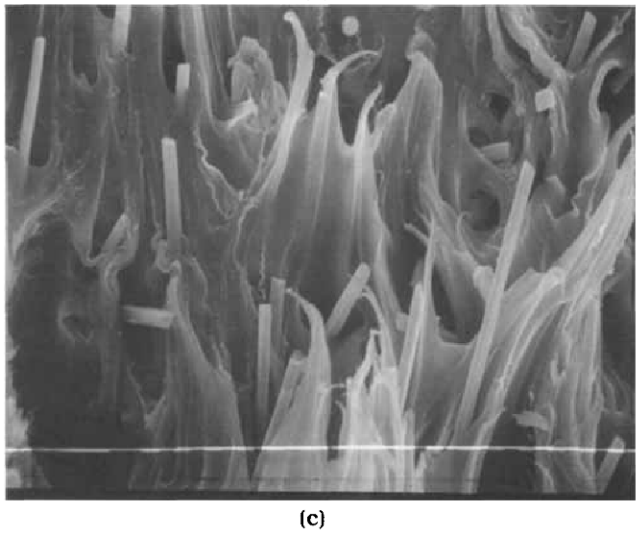

(c)

Fig. 11. Scanning electron micrographs of fracture surface of iPP carbon reinforced samples with different Mw: a) iPP1FC 320×; b) iPP3FC 320×; c) iPP4FC 320×.

weakened fibers, indicating a strong stress exposure during the tensile tests (see *Fig. 12b*); on the contrary, in the sample iPP2FK (see *Fig. 12a*), the Kevlar fibers appear less stressed and unbroken.

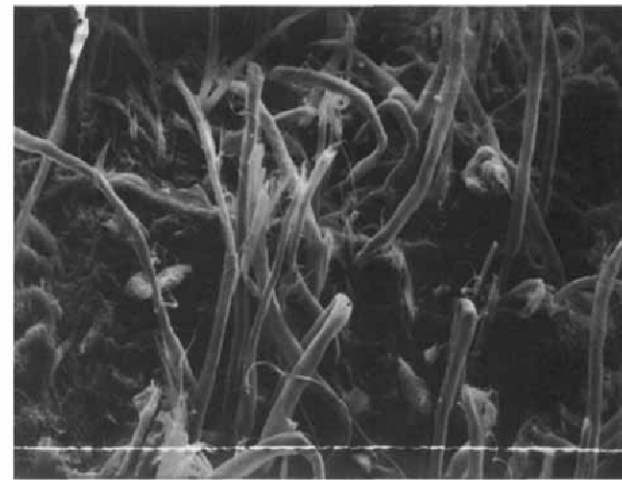

(a)

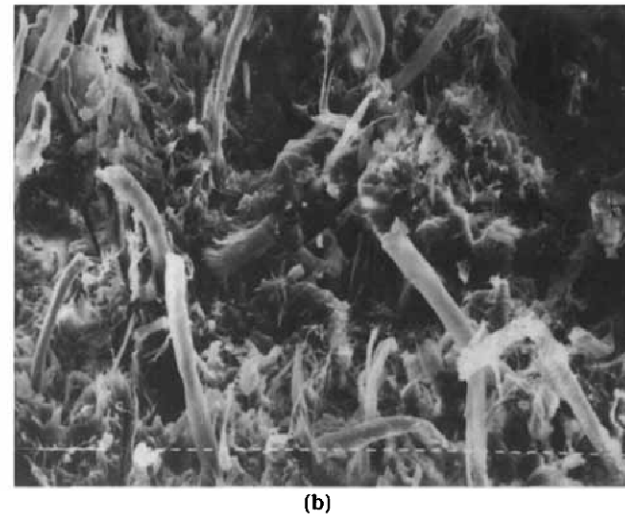

(b)

Fig. 12. Scanning electron micrographs of fracture surface of iPP Kevlar reinforced iPP with different Mw *and crystallization procedures: a) iPP2FK 160×; b) sample iPP4SK 160×.*

ACKNOWLEDGMENTS

We are grateful to Mr. Giuseppe Orsello for his help in the experimental work with the SEM.

This work was partially supported by "Progetto Finalizzato Chimica Fine II-C.N.R."

REFERENCES

1. M. Avella, R. dell'Erba, L. D'Orazio, and E. Martuscelli, (accepted by *Polymer Networks and Blends*, ChemTec Publishing Canada).
2. M. Avella, R. dell'Erba, E. Martuscelli, and G. Ragosta, *Polymer*, **34,** 2951 (1993).
3. M. Avella, E. Martuscelli, B. Pascucci, and M. Raimo, *Polym. Eng. Sci.*, **32,** 383 (1992).
4. C. N. Velisaris and J. C. Seferis, *Polym. Eng. Sci.*, **26,** 1574 (1986).
5. A. M. Chatterjee and F. P. Price, *J. Polym. Sci. Polym. Phys.*, **13,** 2369 (1975).
6. B. Wunderlich, *Macromolecular Physics*, Academic Press, New York (1976).
7. J. Brandrup and E. M. Immergut, *Polymer Handbook*, Vol. 24, Interscience Publishers, New York (1975).

8. M. Avella, G. Della Volpe, E. Martuscelli, and M. Raimo, *Polym. Eng. Sci.*, **32,** 376 (1992).
9. J. D. Hoffmann and J. I. Lauritzen. *J. Appl. Polym. Phys.*, **44,** 4430 (1973).
10. G. V. Fraser, A. Keller, and J. A. Odell, *J. Appl. Polym. Sci.*, **22,** 2079 (1978).
11. L. Mandelkern, *Crystallization in Polymers*, McGraw-Hill, New York (1964).
12. E. Martuscelli, M. Pracella, M. Avella, R. Greco, and G. Ragosta, *Makrom. Chem.*, **181,** 957 (1980).
13. J. D. Hoffmann, *SPE. Trans*, **4,** 315 (1964).
14. H. D. Keith, F. J. Padden, Jr., and G. Vadimsky, *J. Polym. Sci., A-2*, **4,** 267 (1966).
15. A. Lovinger and M. L. Williams, *J. Appl. Polym. Sci.*, **25,** 1703 (1980).
16. J. L. Way, J. R. Atkinson, and J. Weitting, *J. Mater. Sci.*, **9,** 293 (1974).
17. L. W. Kleiner, M. R. Radloff, J. M. Schultz, and T. W. Chon, *J. Polym. Sci. Polym. Phys.*, **12,** 819 (1974).

Revised March 1995